(Invited Paper)

Operational Insight of Microstrip Resonators Using Stepped Impedance Transmission Line and Coupled Lines

Apisak Worapishet
Mahanakorn Microelectronics Research Centre (MMRC)
Mahanakorn University of Technology, Nongchok, Bangkok 10530, Thailand
E-mail: apisak@mut.ac.th

Manuscript received May 10, 2012
Revised May 28, 2012

ABSTRACT

An operational insight of the Microstrip resonator using the stepped impedance transmission line and the recently introduced stepped impedance coupled lines is outlined in this paper. This qualitative description is based upon phasor diagrams of waves propagating along a lossless stepped impedance open-ended line. In essence, it visualizes how the first parallel resonance frequency of the stepped impedance resonator can be shifted up to a higher frequency, or down to a lower frequency, as compared to that of its uniform impedance counterpart. In summary, It is found that the stepped impedance resonator relies upon the use of partial reflections at the stepped impedance junctions between the transmission line sections to perturb the phase shift of the wave propagating one-round along the line, thereby effectively modifying the resonance frequency. Such insightful understanding also brings to light the underlying operation of transmission line perturbation structures in general, and these can be useful for performance enhancement of other microwave circuit building blocks.

Keywords: *Stepped impedance transmission lines, Stepped impedance coupled lines.*

1. INTRODUCTION

The stepped impedance transmission line technique has been widely employed to enhance performances of numerous microwave circuits. One of its major applications includes the parallel-coupled Microstrip bandpass filters [1] which inevitably suffer from the spurious response at twice the fundamental passband frequency. This is due to the difference between the modal phase velocities in the dielectric medium of the coupled Microstrip lines which is intrinsically inhomogeneous, causing the odd mode to propagate faster than the even mode. To alleviate this problem, it was demonstrated in [2] that the first parallel resonance frequency of a stepped impedance transmission line resonator can be *shifted* via adjustment of the stepped impedance ratio between the transmission line sections, and hence the stepped impedance technique can be employed to push the locations of the spurious frequency bands to higher frequencies [2] - [5].

It is not until recently that the concept of the stepped impedance transmission line has been extended to parallel coupled lines. In [6], it was demonstrated the incorporation of the stepped impedance structure into a coupled Microstrip resonator enables us to align the even- and odd-mode resonance frequencies by appropriate selections of the stepped impedance ratios in each mode. This effectively equalizes the modal phase velocities with the consequent benefit to considerable spurious response suppression in the parallel-coupled Microstrip bandpass filters. It was also verified in [6] that the stepped impedance coupled line enables closed-form analysis, as well as simple design and implementation.

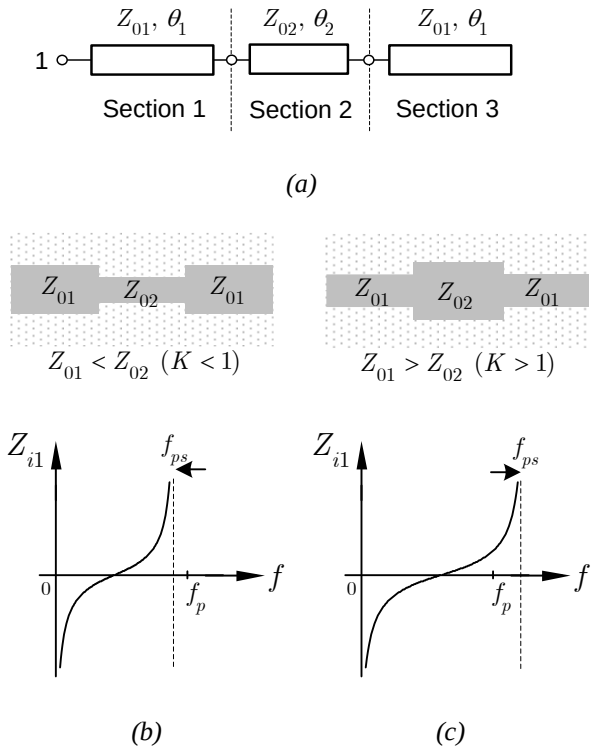

Fig. 1 *Stepped impedance resonator. (a) Circuit schematic, and Microstrip layouts at (b) $Z_{01} < Z_{02}$ (K<1) and (c) $Z_{01} > Z_{02}$ (K>1).*

In spite of their popularity, the underlying physical insight into the operation of the stepped impedance transmission line and coupled line structure has not yet been explored. So far in the literature, only mathematical analysis of the stepped impedance structures has been given and this provides no insight into the operation – how the resonance frequency can be shifted towards high and low frequency by virtue of the stepped impedance ratios between the transmission line sections. Understanding this underlying physical mechanism should prove very useful to expanding its future applications. It is thus the purpose of this paper to bring to light an operational insight of the stepped impedance transmission lines and coupled lines.

2. STEPPED IMPEDANCE RESONATORS AND THEIR QUALITATIVE OPERATION

A. Overview

The schematic of the open-ended stepped impedance resonator or SIR is shown in Fig. 1(a) where it is formed by a cascade of three transmission line sections 1, 2 and 3 with the characteristic impedances Z_{01}, Z_{02} and Z_{01}, and the electrical lengths θ_1, θ_2 and θ_1, respectively [2].

By virtue of the stepped impedances of the transmission line sections, the first *parallel* resonance frequency of the *stepped* impedance resonator, f_{sp}, can be adjusted as compared to the *parallel* resonance frequency of its *uniform* impedance counterpart, f_p, with $Z_{01} = Z_{02}$ or $K = 1$, where $K = Z_{01} / Z_{02}$ is the stepped impedance ratio. It is important to note that this can also be viewed as adjustments of the *effective* phase constant β_s^{ef} and phase velocity v_s^{ef} of the stepped impedance line, as will be evident later. In the case that $Z_{01} < Z_{02}$ or $K < 1$ as shown in Fig. 1(b) for a stepped impedance Microstrip line, the resonance frequency f_{sp} is moved to a lower frequency than that of its uniform counterpart at f_p. This indicates that the effective phase constant β_s^{ef} is higher, and that the effective phase velocity v_s^{ef} is slower. For the opposite case when $Z_{01} > Z_{02}$ or $K > 1$ in Fig. 1(c), f_{sp} is moved to a higher frequency than f_p. Thus, the phase constant β_s^{ef} is lower and the phase velocity v_s^{eff} is faster.

Having provided the overview of the SIR characteristic, we are now ready to describe the operational principle of the stepped impedance coupled resonator or SICR. Let us consider the schematics of the symmetric open-ended *uniform* impedance coupled Microstrip resonator when it is decomposed into a superposition of the even- and odd-mode excitations as shown in Fig. 2. As evident, because the field configurations are different due to the air-dielectric interface, the effective dielectric constants of the two excitation modes are different. As a consequence, the phase constants, phase velocities, and parallel resonance frequencies in the even and odd modes are different, giving rise to spurious response around the resonance frequency when employed in coupled Microstrip filters.

Another important observation from the modal decomposition of the Microstrip coupled resonator in Fig. 2 is the fact that it can actually be treated as a *single* transmission line under each excitation mode. Such recognition is of crucial significance since it enables us to extend the concept of the SIR to each of the modal transmission lines. In particular, the resonance frequencies in the even and odd modes, f_{spe} and f_{spo}, of the *stepped* impedance coupled resonator can be aligned by appropriate selection of the modal characteristic impedances, $Z_{01e,02e}$ and $Z_{01o,02o}$. This essentially equalizes the effective modal phase velocities, v_{se}^{ef} and

v_{so}^{ef}, and the effective modal phase constants, β_{se}^{ef} and β_{so}^{ef}, of the stepped impedance coupled lines, with consequent benefit to suppressing the first harmonic spurious response in the SICR. The detailed analysis of the SICR can be found in [6].

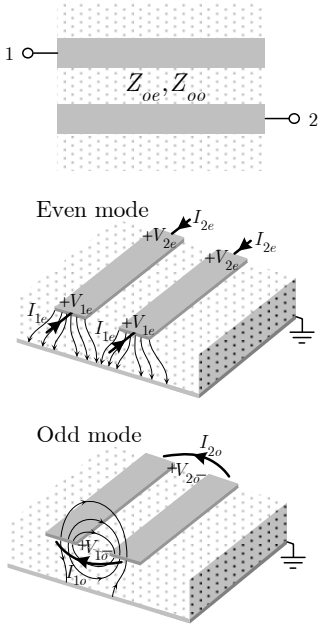

Fig. 2 *Open-ended coupled Microstrip resonator under even-mode and odd-mode excitations, with outlines of field configurations [6].*

Fig. 3(a) shows the schematic of the stepped impedance coupled lines. It is essentially formed by a cascade of three coupled line sections 1, 2, and 3. Sections 1 and 3 are identical. Their even- and odd-mode characteristic impedances are at Z_{0e1} and Z_{0o1}, and the electrical lengths at θ_{e1} and θ_{o1}, respectively. For section 2, the modal characteristic impedances are at Z_{0e2} and Z_{0o2}, and the electrical lengths at θ_{e2} and θ_{o2}. Note that the step impedance ratio in each mode is defined by $K_{e,o} = Z_{0e1,o1} / Z_{0e2,o2}$. For a conventional coupler with a uniform coupled line, we have $K_e = K_o = 1$.

The incorporation of the stepped impedance structure into coupled Microstrip lines to form the stepped impedance couplers enables us to align the even- and odd-mode phase velocities by appropriate selections of the modal stepped impedance ratios $K_{e,o}$. Fig. 3 illustrates three possible outlines of the layouts for the odd- and even-mode resonance frequency alignment in the SICR. As described in [6], the layout with $K_{e,o} < 1$ requires less impedance steps in each mode. Thus, its layout should suffer less impact non-ideal effects such as discontinuities at the stepped impedance transitions.

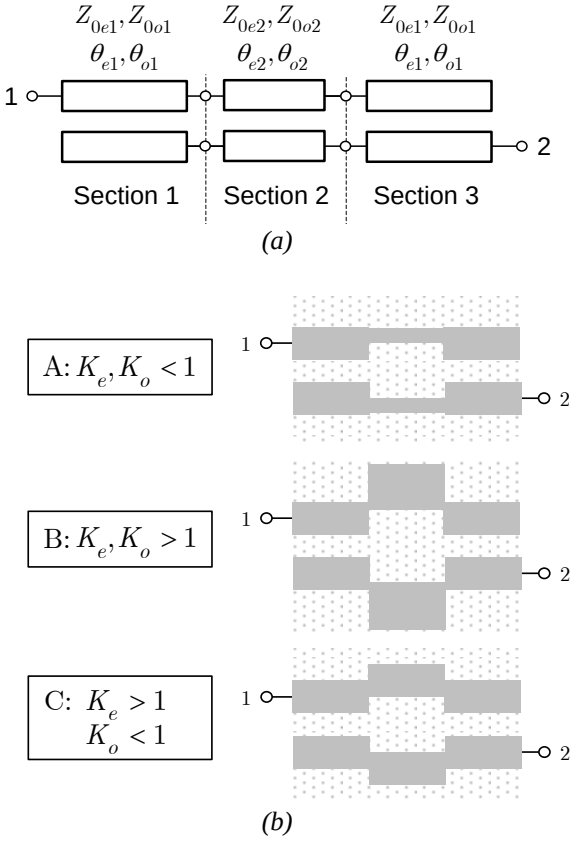

Fig. 3 *Stepped impedance coupled resonator. (a) Circuit schematic, and (b) Microstrip layouts at different modal impedance ratios, K_e and K_o [6].*

B. Operational Principle of the SIR and SICR

The principal operation of the stepped impedance resonator is provided in this section through an insightful description based on phasor diagrams of *current* waves propagating along a lossless stepped line as shown in [7]. In essence, it will be described in a qualitative manner how the resonance frequency can be moved up to a higher frequency, or down to a lower frequency, as compared to that of the uniform impedance resonator, by virtue of the stepped impedances of the transmission line sections that form the SIR and SICR. Since the SICR relies upon the operation of the SIR for the odd- and even-mode resonance frequency alignment, only the SIR description suffice to provide an insightful operation for both resonators. Unless stated otherwise, our main focus is on the first *parallel* resonance characteristic.

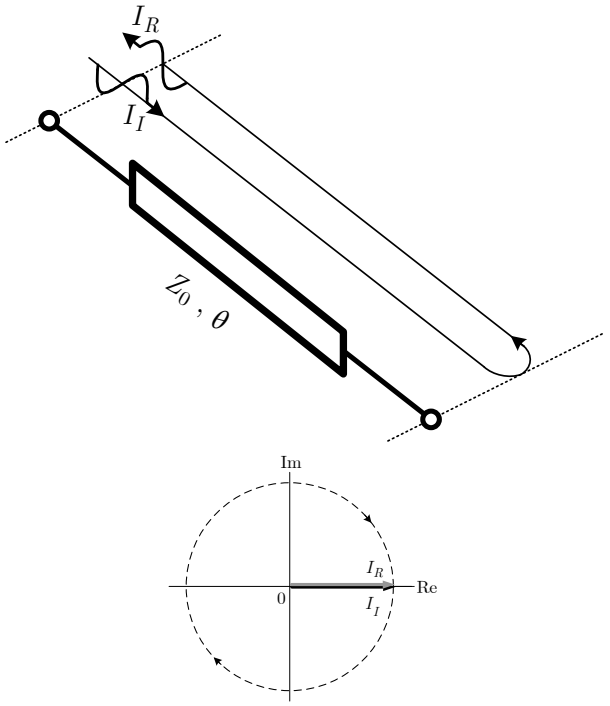

Fig. 4 *Uniform impedance resonator and phasor diagram of travelling waves at resonance frequency after travelling one round on the transmission line.*

To facilitate the description that follows, we first consider the uniform impedance resonator at the resonance frequency f_p, as shown in the schematic of Fig. 4. Also given in the figure is the phasor diagrams of the reflected wave I_R and the incident wave I_I after it propagated towards the open-end, undergone a total reflection and travelled back to the input end. At f_p, the total phase shift ϕ_T associated with this reflected wave I_R travelling one round, with reference to the incident wave I_I, is $\phi_T = -2\pi$. As a consequence, I_R and I_I are in phase and this results in a complete cancellation between the reflected and incident *current* waves at the input end, yielding a zero input admittance $Y_i = 0$, or equivalently an infinite input impedance $Z_i = \infty$, in accordance with the parallel resonance condition.

Let us now consider the stepped impedance resonator of Fig. 5(a) which is formed by a cascade of three transmission line sections 1, 2 and 3 with the characteristic impedance Z_{01}, Z_{02} and Z_{01}, respectively [2]. Without loss of generality, the electrical length associated with each section is assumed identical at θ, where $\theta = \pi/3$ at the frequency f_p.

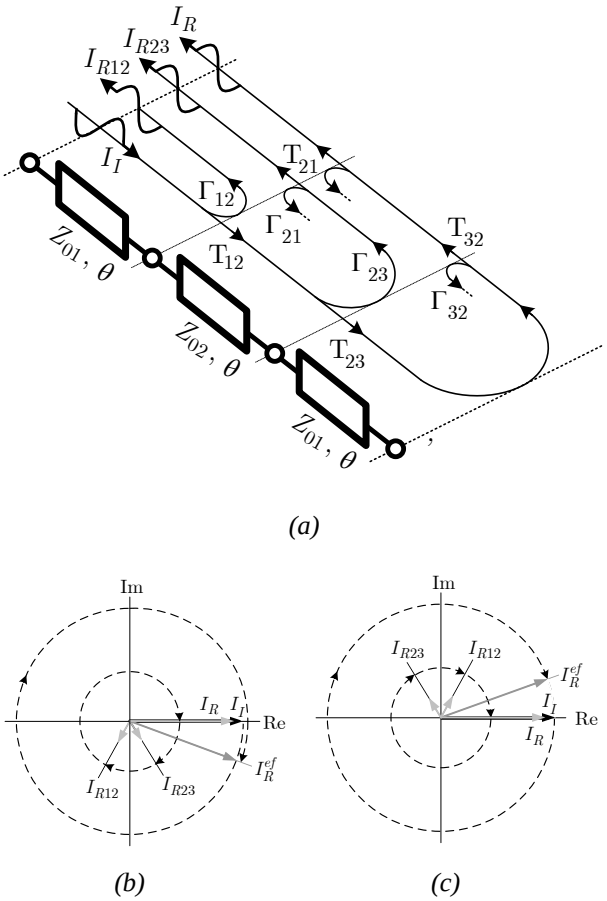

Fig. 5 *Stepped impedance resonator (a) Partial reflections and transmissions, (b) and (c) phasor diagrams of waves travelling on SIR when $\Gamma>0$ and $\Gamma<0$ [see text for the definition of Γ].*

To simplify the description, it is utilized here the theory of small reflection [8], which approximates multiple reflections of a wave at discontinuities between different impedances by the first reflections. Although the result is only accurate under a small reflection, the operational insight obtained from this approximation is general and can be applied for the SIR with a large reflection. For the resonator in Fig. 5(a), the partial reflections and transmissions of the travelling wave are illustrated in Fig. 5(a), where the reflection and transmission coefficients (Γ's and T's) are given by

$$\Gamma_{12} = \Gamma_{32} = -\Gamma_{23} = -\Gamma_{21} = \frac{Z_{02} - Z_{01}}{Z_{02} + Z_{01}} = \frac{1-K}{1+K} \quad (1)$$

$$\mathrm{T}_{12} = \mathrm{T}_{32} = 1 - \Gamma_{12} = \frac{2Z_{01}}{Z_{02} + Z_{01}} = \frac{2}{1 + 1/K} \tag{2}$$

$$\mathrm{T}_{21} = \mathrm{T}_{23} = 1 + \Gamma_{12} = \frac{2Z_{02}}{Z_{02} + Z_{01}} = \frac{2}{1 + K} \tag{3}$$

where $K = Z_{01} / Z_{02}$ is the impedance ratio. By invoking the theory of small reflection and using (1) to (3), the *effective* reflected wave I_R^{ef} at the input end of the resonator can be given, at the resonance frequency f_p of its *uniform* counterpart, by

$$\begin{aligned} I_R^{ef} &= \Gamma_{12} e^{-j\frac{2\pi}{3}} + \mathrm{T}_{12}\Gamma_{23}\mathrm{T}_{21} e^{-j\frac{4\pi}{3}} + \mathrm{T}_{12}\mathrm{T}_{23}\mathrm{T}_{32}\mathrm{T}_{21} e^{-j2\pi} \\ &= \underbrace{\Gamma e^{-j\frac{2\pi}{3}}}_{1st\ \text{term}} - \underbrace{\Gamma(1-\Gamma^2) e^{-j\frac{4\pi}{3}}}_{2\text{nd term}} + \underbrace{(1-\Gamma^2)^2 e^{-j2\pi}}_{3rd\ \text{term}} \end{aligned} \tag{4}$$

where we set $\Gamma_{12} = \Gamma$ for brevity. Also, a unit amplitude is assumed for the incident current wave. Note that the first and second terms in (4) represent the partially reflected waves at the step impedance junctions, whereas the third term represents the transmitting wave that travels one complete round on the SIR [cf. Fig. 5(a)].

Consider the case that $Z_{01} < Z_{02}$ or $K < 1$ and that the positive reflection coefficient is assumed at $\Gamma = +0.1$. With the use of (4), the phasor diagrams of the *effective* reflected wave I_R^{ef} and the incident wave I_I at the frequency f_{pu} can be shown in Fig. 5(b). As indicated, I_R^{ef} lags behind I_I by *more* than -2π rad. This implies that the effective phase constant β^{ef} of the stepped impedance line with $K < 1$ is higher than that of the uniform line with $K = 1$. Thus, the effective phase velocity v_p^{ef} is slower, indicating that the resonance frequency f_{ps} of the SIR is moved to a lower frequency than f_p. This can also be explained as follows. At the resonance frequency f_{ps} where a complete cancellation between the effective reflected wave I_R^{ef} and the incident current wave I_I takes place, the phase shift ϕ associated with each transmission line section is *smaller* than $2\pi/3$ rad, i.e., $\phi < 2\pi/3$. Since phase shift and frequency of a wave on a transmission line are in direct proportion, f_{ps} is lower than f_p as a result.

For the opposite case when $Z_{01} > Z_{02}$ or $K > 1$, the phasor diagrams of I_R^{ef} and I_I at the frequency f_p are shown in Fig. 5(c) where $\Gamma = -0.1$ is assumed. Since I_R^{ef} lags behind I_I by *less* than -2π rad, the effective phase constant β^{ef} is smaller and the phase velocity v_p^{ef} is faster. Also, the phase shift ϕ associated with each transmission line section at the resonance frequency f_{ps} of the SIR is *larger* than $2\pi/3$ rad, and thus f_{ps} is moved to a higher frequency than f_p.

To summarize the operation, it can be deduced that the SIR relies upon the use of partial reflections at the stepped impedance junctions of the transmission line sections to perturb the phase shift of the transmitting wave that propagates one complete round on the resonator. As a consequence, under the resonance condition when the effective reflected wave and the incident current wave cancel out, the phase shift associated with each transmission line section of the SIR is modified from the case of the uniform impedance resonator. Therefore, the parallel resonance frequency is shifted from that of the uniform resonator, and can be adjusted by the impedance steps between sections. Note that this can also be viewed as a change in the effective phase constant and phase velocity of the stepped impedance line.

3. CONCLUSION

By using simple phasor diagrams illustrating waves propagating along a lossless stepped impedance open-ended line, the qualitative operation of the stepped impedance resonator, either of transmission line and coupled line types, has been visualized. It is evident from the operation that the stepped impedance resonator relies upon the partial reflections resulting from the perturbation at the stepped impedance junctions between the transmission line sections. This essentially changes the phase shift of the wave propagating one-round along the line, thereby effectively modifying the resonance frequency to a higher or lower frequency depending on the step impedance ratio.

With such understanding, it is envisaged that other perturbation schemes, such as those employing lumped/distributed capacitors or inductors along a uniform transmission line can be employed to provide similar resonance frequency shifting property. Thus, these capacitive and inductive perturbation structures can also offer even- and odd-mode phase velocity equalization in coupled lines and hence spurious frequency suppression in parallel-coupled line Microstrip filters. Finally, it is important to note that the analysis approach based upon the theory of small reflection as presented here is general and can potentially be extended to analyze generalized transmission line perturbation structures. This is the subject of our current investigation.

REFERENCES

[1] S. B. Cohn, "Parallel-coupled transmission line, " *IRE Trans. Microw. Theory Tech.*, vol. MTT-6, no. 2, pp. 223-231, Apr. 1958.

[2] M. Makimoto and S. Yamashita, "Bandpass filters using parallel coupled stripline stepped impedance resonators," *IEEE Trans. Microw. Theory Tech.*, vol. MTT-28, no. 12, pp. 1413-1417, Dec. 1980.

[3] J.-T. Kuo, E. Shih, "Microstrip stepped impedance resonator bandpass filter with an extended optimal rejection bandwidth," *IEEE Trans. Microw. Theory Tech.*, vol. 51, no. 5, pp. 1554-1559, May 2003.

[4] C.-F. Chen, T.-Y. Huang, R.-B. Wu, "Design of microstrip bandpass filters with multi-order spurious-mode suppression," *IEEE Trans. Microw. Theory Tech.*, vol. 53, no. 12, pp. 3788-3793, Dec. 2005.

[5] S.-C. Lin, P. –H. Deng, Y.-S. Lin, C.-H. Wang, C. H. Chen, "Wide-stopband microstrip bandpass filters using dissimilar quarter-wavelength stepped-impedance resonators," *IEEE Trans. Microw. Theory Tech.*, vol. 54, No. 3, pp. 1011 – 1018, Mar. 2006.

[6] A. Worapishet, K. Srisathit, W. Surakampontorn, "Stepped Impedance Coupled Resonators for Implementation of Parallel Coupled Microstrip Filters With Spurious Band Suppression," *To appear in IEEE Trans. Microw. Theory Tech.*

[7] A. Worapishet, *Wireless CMOS Integrated Circuit Techniques*, Bangkok, Mahanakorn University Press, 2010, Chapter. 4.

[8] D. M. Pozar, *Microwave Engineering*, 3rd ed. New York: Wiley, 2003, Chapter. 5.

Apisak Worapishet received the B.Eng. degree (with first-class honors) from King Mongkut's Institute of Technology Ladkrabang, Bangkok, Thailand, in 1990, the M.Eng.Sc. degree from the University of New South Wales, Australia, in 1995, and the Ph.D. degree from Imperial College, London, U.K., in 2000, all in electrical engineering. Since 1990, he has been with Mahanakorn University of Technology, Bangkok, Thailand, where he currently serves as the Director of Mahanakorn Microelectronics Research Center (MMRC). He is also a Professor in the Telecommunication Department. His current research interest includes mixed-signal CMOS analog integrated circuits, wirelined and wireless RF CMOS circuits, microwave circuits.